Simulation of Electrostatic Noise Amplification in Gyrotrons

KWO RAY CHU, SENIOR MEMBER, IEEE, AND LING-HSIAO LYU

Abstract—**Electrostatic noise generated by the electrostatic cyclotron instability is simulated in slab geometry with dc space charge effects neglected. The noise is found to be characterized by a broad spectrum, low saturation levels, and a strong disturbing effect on the electron energy distribution.**

I. INTRODUCTION

IN THE CONVENTIONAL O-type microwave tubes, the electrons move in straight trajectory through the interaction structure. An observer moving along with the beam (i.e., in the beam frame) sees a stationary beam and hence no kinetic energy. This argument proves that the beam can not sustain a growing wave (an instability) by itself without coupling to the modes of the external interaction structure. In reality, the beam is coupled with the modes of a nonuniform interaction structure (e.g., a helical waveguide). When viewed in the beam frame, microwave power is derived from the kinetic energy associated with the backward motion of the external structure. A more complex situation exists in the gyrotron where beam electrons follow helical orbits along an applied magnetic field. The axial kinetic energy may disappear in some reference frame, but the gyrational kinetic energy persists in all frames. Hence, an instability can in principle exist as a pure beam mode without any coupling to the external structure.

One such possibility, the electrostatic cyclotron instability (ESCI), has been analyzed by several authors [1]–[3]. This instability is due to the same relativistic bunching mechanism that drives the cyclotron maser instability in a gyrotron. The difference lies in the nature of the wave. The cyclotron maser instability involves the electromagnetic modes of the interaction structure, while the ESCI involves electrostatic modes of the beam that propagate principally in the direction transverse to the applied magnetic field.

Reference [1] develops a simple macroscopic model of the ESCI where the finite electron Larmor radius effects, and hence the nonfundamental cyclotron harmonic modes are neglected. It points out that this instability may lead to noise amplification in gyrotrons. Reference [2] treats the ESCI as a potential radiation mechanism, thus emphasizing its coupling with the electromagnetic modes of the interaction structure. Reference [3] studies the ESCI principally in the context of noise amplification. Effects neglected in [1], but of importance to noise analysis (such as the multimode and multiharmonic nature), are therefore stressed. It is shown [3] that an electrostatic perturbation on the beam can be amplified as microscopic beam modes at a rate comparable to the RF signal amplification in gyrotron amplifiers. Further, modes with the greatest growth rates are completely localized within the beam and hence can grow in drift regions as well as in cavities and waveguides. These facts raise the concern that the ESCI will enhance the initial noise to a level unacceptable for some contemplated applications of gyrotrons (e.g., deep space communication) and that it will degrade the beam quality to result in lower than expected RF gain and efficiency.

Theories on ESCI have so far been conducted in the small-signal regime and hence provide no quantitative insights to these possible deleterious effects. The present paper investigates the ESCI in the large-signal regime. Computer simulations are made for a moderate-power (~ 1 MW) and a high-power (~ 100 MW) gyrotron beam. In both cases, it is found that the noise spectrum is rich in spatial Fourier components and temporal cyclotron harmonics. The saturated wave energy density is low compared with the beam energy density, but there is a strong disturbing effect on the beam quality. Following a brief summary of the small-signal theory in Section II, details of the simulation results are presented.

II. REVIEW OF THE SMALL-SIGNAL THEORY

Our model consists of a neutral, uniform, and infinite plasma immersed in an external magnetic field $B_0 e_z$. We are concerned with high-frequency electrostatic modes which propagate across the magnetic field with $\exp(ik_x x - i\omega t)$ dependence. It is well known that if the electrons are cold, such modes reduce to oscillations at the upper hybrid frequency. If the electrons are warm with a Maxwellian distribution, there then exist a multitude of electrostatic modes at approximately the upper hybrid frequency and the nonfundamental harmonics of the cyclotron frequency, known as the Bernstein modes. The present work specializes to a distribution function representative of the

Manuscript received August 27, 1985; revised January 23, 1986. This work was supported in part by the National Science Council of the Republic of China.

The authors are with the Department of Physics, National Tsing Hua University, Hsinchu, Taiwan, Republic of China.

IEEE Log Number 8607966.

electron beam in a gyrotron

$$f = \frac{1}{2\pi p_\perp}\delta(p_\perp - p_{\perp o})\delta(p_z - p_{zo}) \tag{1}$$

where $p_\perp$ and p_z are, respectively, the electron momentum perpendicular and parallel to the magnetic field, and $p_{\perp o}$ and p_{zo} are their initial values (same for all electrons). Then, for sufficiently large $p_{\perp o}$ (see (5)), the Bernstein modes become unstable and the branch that has the upper hybrid frequency now centers at the fundamental cyclotron frequency. The dispersion relation is [3]

$$1 - \frac{\pi_{pe}^2 V_n}{\omega^2 - n^2\Omega_c^2} + \frac{2\pi_{pe}^2(\omega^2 + n^2\Omega_c^2)U_n}{(\omega^2 - n^2\Omega_c^2)^2} = 0 \tag{2}$$

where

$$V_n \equiv n\left[J_{n-1}^2(k_x r_{Lo}) - J_{n+1}^2(k_x r_{Lo})\right] \tag{3}$$

$$U_n \equiv J_n^2(k_x r_{Lo}) n^2\Omega_c^2/(k_x^2 c^2) \tag{4}$$

n is the cyclotron harmonic number, r_{Lo} is the initial electron Larmor radius, π_{pe} and Ω_c are, respectively, the relativistic plasma frequency and relativistic cyclotron frequency of electrons with the initial relativistic factor $\gamma_o = [1 + (p_{\perp o}^2 + p_{zo}^2)/m_e^2 c^2]^{1/2}$.

Writing $\omega = \omega_r + i\omega_i$ (with $\omega_i \ll \omega_r$) and assuming

$$\pi_{pe}^2 < \frac{16 n^2\Omega_c^2 U_n}{(V_n - 2U_n)^2} \tag{5}$$

we obtain from (2) the solution

$$\omega_r \simeq n\Omega_c\left[1 + \frac{\pi_{pe}^2}{2n^2\Omega_c^2}(V_n - 2U_n)\right]^{1/2} \tag{6}$$

and

$$\omega_i \simeq \pi_{pe}\left[U_n - \frac{\pi_{pe}^2}{16 n^2\Omega_c^2}(V_n - 2U_n)^2\right]^{1/2}. \tag{7}$$

In the limit $\pi_{pe}^2 \ll n^2\Omega_c^2$, (6) and (7) reduce to

$$\omega_r \simeq n\Omega_c\left[1 + \frac{\pi_{pe}^2}{4n^2\Omega_c^2}(V_n - 2U_n)\right] \tag{8}$$

and

$$\frac{\omega_i}{\Omega_c} \simeq \beta_{\perp o}\frac{\pi_{pe}}{\Omega_c}\left|\frac{nJ_n(k_x r_{Lo})}{k_x r_{Lo}}\right| \tag{9}$$

where $\beta_{\perp o}$ is the initial perpendicular velocity divided by the speed of light.

III. The Simulation Code and Model

A one-dimensional electrostatic code [4] has been used to simulate the system described in Section II. However, the simulated system is assumed to be periodic in x with period $2d$, hence only modes with

$$k_x = \frac{m\pi}{d}, \qquad |m| = 1, 2, 3, \cdots \tag{10}$$

are excited. Good numerical convergence is obtained with 32 uniformly spaced grid points per spatial period and 200 simulation particles per grid.

Two cases have been simulated: (I) $\beta_{\perp o} = 0.4$, $\pi_{pe}/\Omega_c = 0.05$, and (II) $\beta_{\perp o} = 0.8$, $\pi_{pe}/\Omega_c = 0.1$. In both cases, we assume $d = 3r_{Lo}$ and $\beta_{zo} = 0$, hence in (9)

$$k_x r_{Lo} = \frac{m\pi}{3}. \tag{11}$$

At this point, it is appropriate to consider the relevance of the simulated system to the electron beam in an actual gyrotron.

The electrostatic approximation is valid when

$$k_x^2 c^2 \gg \pi_{pe}^2.$$

This is a condition generally satisfied in gyrotrons. Here, for example, we have $k_x c/\pi_{pe} > 50$ and 13 for Case I and Case II, respectively. As a double check, we have simulated Case II, for which the electrostatic condition is less satisfied with an electromagnetic simulation code. The results are essentially the same.

The simulation is done with a one-dimensional code because of the assumption $k_z = 0$. This is an acceptable simplification because $k_z = 0$ modes are the most unstable as compared with the $k_z \neq 0$ modes [3]. In reality, however, the axial wavelength must be finite.

The model of an infinite and uniform plasma is unrealistic, but not as drastically as it first appears. For an initial perturbation, which is symmetric about $x = 0$, traveling waves in positive and negative x-directions will be generated with equal amplitude, resulting in a standing wave pattern. The distance between the nodes is d (half of the spatial period). It can be easily seen that the total perturbed charge vanishes in the plasma slab between the nodes. Gauss' law then states that each plasma slab is independent of the other, because the electric field produced by each slab vanishes outside the slab. Thus, with the imposition of the periodic condition and symmetric initial condition, we are effectively simulating a plasma slab of thickness d, which has been taken to be three Larmor radii in Cases I and II. As for the unrealistic aspects, the simulated plasma slab is in the Cartesian geometry with sharp boundaries, whereas the actual electron beam is cylindrical with diffusive boundaries. Furthermore, by assuming a charge neutral plasma, we have neglected the dc space charge effects.

Finally, we point out that the simulation is done in the beam reference frame ($\beta_{zo} = 0$). When transformed into the lab frame where the beam has $v_{\perp o}/v_{zo} = 1.5$, Case I approximately corresponds to a 70-kV, 1-MW annular electron beam in a fundamental harmonic gyrotron, while Case II approximately corresponds to the 500-kV, 100-MW electron beam in the University of Maryland gyroklystron amplifier design [5], which is expected to produce 30-MW peak power in the X band.

IV. Analytical Predictions and Simulation Results

We introduce the following notations:

$E(x,t)$ Electric field as a function of x and t.
$E(m,t)$ Fourier transform of $E(x,t)$ in space.
$E(m,\omega)$ Fourier transform of $E(x,t)$ in space and time.
W_E Total electric field energy in the plasma slab averaged over one cyclotron period.
W_{eo} Total initial electron kinetic energy in the plasma slab.
$\Delta\gamma$ $\gamma(t)-\gamma_o=$ change of γ from its initial value γ_o.
$\langle\Delta\gamma\rangle$ Root mean square of $\Delta\gamma$ of all electrons (i.e., standard deviation of γ from γ_o).

The base period for the spatial Fourier transform is $2d$ as noted before. The base period for Fourier transform in time is typically several tens of cyclotron periods, hence the spectrum in ω approaches a continuum.

A. Analytical Predictions

The small-signal gain per cyclotron period is

$$g_c = 20\log\frac{|E(m,t+\tau_c)|}{|E(m,t)|} = 20\log e^{2\pi\omega_i/\Omega_c} = 54.6\frac{\omega_i}{\Omega_c}\text{dB} \quad \text{(per cyclotron period)} \qquad (12)$$

where $\tau_c \equiv 2\pi/\Omega_c$ is the cyclotron period and ω_i/Ω_c is given by (9) and (11). Fig. 1 plots the gain as a function of the cyclotron harmonic number n for different spatial Fourier components of the wave. Note that the spectrum of a higher spatial Fourier component is dominated by a higher cyclotron harmonic, while the overall spectrum is dominated by the $n=m=1$ mode. The simultaneous presence of many unstable modes marks another difference between the ESCI and the electromagnetic cyclotron instability in a gyrotron. The magnetic field in a gyrotron can be tuned to allow a single low-order electromagnetic circuit mode to be unstable, but this is not possible for the electrostatic cyclotron modes.

B. Simulated Noise Spectrum

Fig. 2 plots the spatial Fourier components $[E(m,t)]$ as a function of time in the small signal regime. Each component exhibits an exponential growth rate, with the $m=1$ mode being the fastest growing. High m modes contain more cyclotron harmonics (cf. Fig. 1) and therefore have more complex time dependence.

Fig. 3 shows the cyclotron harmonic composition of the corresponding data in Fig. 2. $E(m,\omega)$ is seen to peak at the harmonics of the cyclotron frequency. The spikes have finite width because a growing mode does not have pure sinusoidal dependence. In fact, the width of the spike is approximately proportional to the growth rate. We note that the relative amplitudes of the spikes are in good

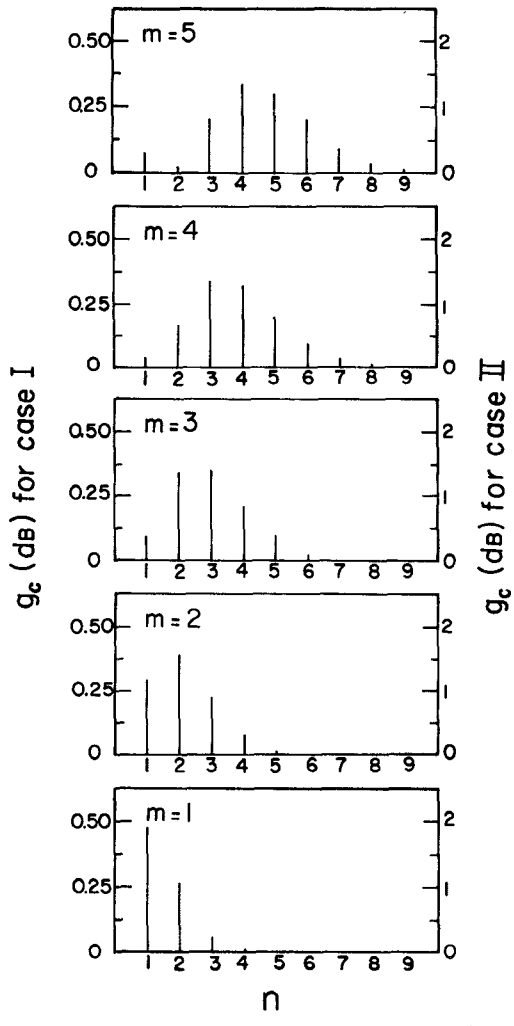

Fig. 1. Analytically evaluated small signal gain per cyclotron period (g_c) as a function of the cyclotron harmonic number n and spatial harmonic number m. The absolute and relative values are both in agreement with simulated results (cf. Figs. 2 and 3).

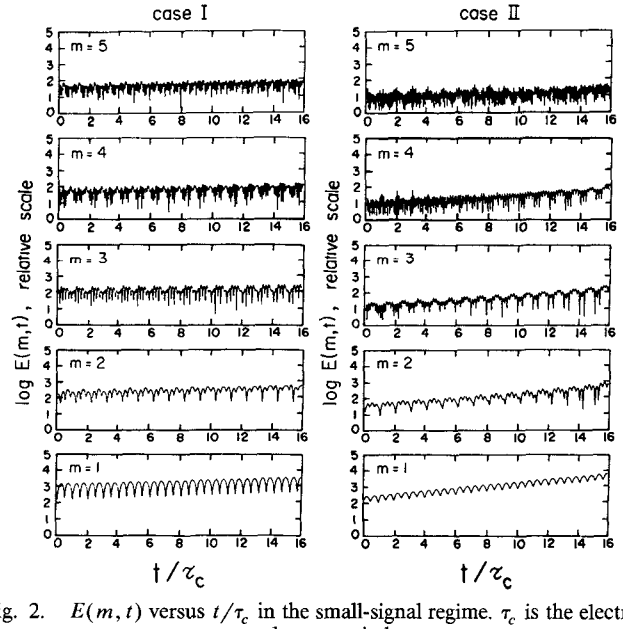

Fig. 2. $E(m,t)$ versus t/τ_c in the small-signal regime. τ_c is the electron cyclotron period.

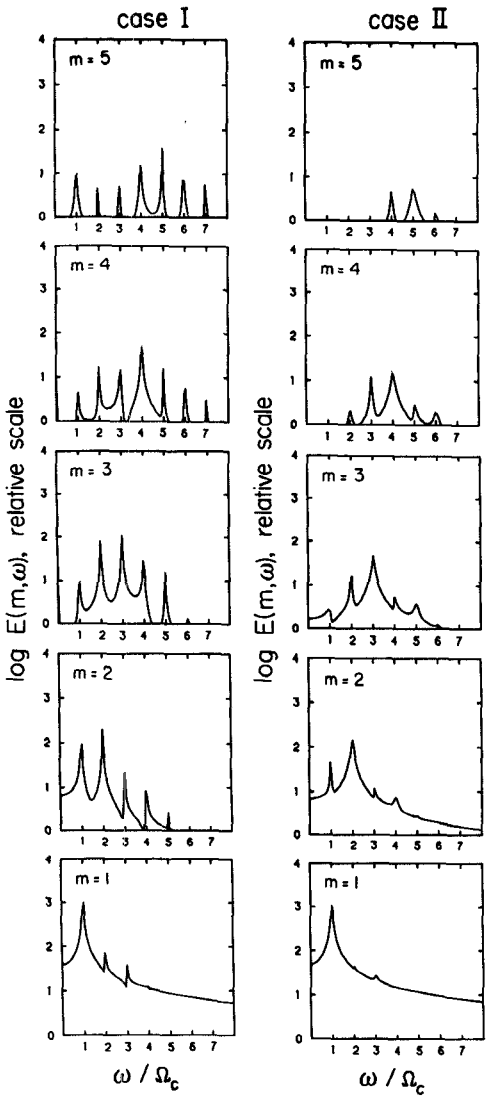

Fig. 3. $E(m,\omega)$ versus ω/Ω_c in the small-signal regime.

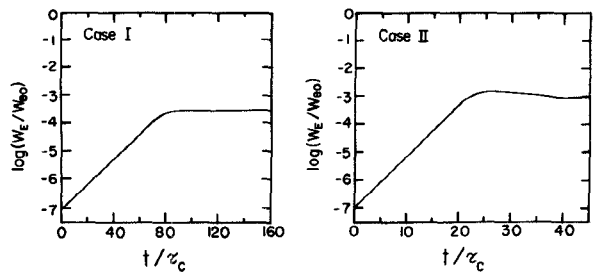

Fig. 4. $\log(W_E/W_{eo})$ versus t/τ_c in the small- and large-signal regimes.

agreement with the theoretical predictions in Fig. 1. In the large signal regime (not plotted), however, the relative amplitudes vary with time, showing the saturation behavior.

C. Saturation Levels and Effect on Beam Quality

Fig. 4 plots $\log(W_E/W_{eo})$ as a function of time (normalized to τ_c). In both cases, the initial noise energy level is assumed to be $W_E/W_{eo}=10^{-7}$. Wave energy first increases exponentially with time (the straight section of the curve).

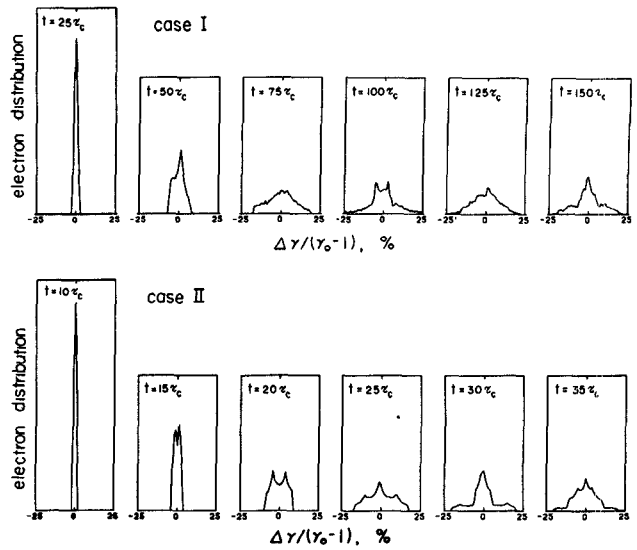

Fig. 5. Evolution of the electron distribution in energy. At $t=0$ (not plotted), all the electrons have the same kinetic energy $(\gamma_o-1)m_ec^2$. At subsequent times, the number of electrons is plotted (in relative linear scale) as a function of the percentage deviation from the initial kinetic energy.

Then, rather suddenly, it saturates (the flat section of the curve). Gain as inferred from the slope of the straight section of the curve is found to be in good quantitative agreement with theoretical predictions for the dominant mode ($m=n=1$), that is

$$g_c \simeq \begin{cases} 0.48 \text{ dB (per cyclotron period)}, & \text{Case I} \\ 1.90 \text{ dB (per cyclotron period)}, & \text{Case II} \end{cases} \quad (13)$$

Saturation level of the wave energy is relatively low

$$\left(\frac{W_E}{W_{eo}}\right)_{\text{sat}} \simeq \begin{cases} 3.5\times10^{-4}, & \text{Case I} \\ 1.5\times10^{-3}, & \text{Case II} \end{cases} \quad (14)$$

which corresponds to the following peak-wave electric-field amplitude (multiplied by the Larmor radius)

$$E_{\text{sat}}r_{Lo} \simeq 1026\frac{\pi_{pe}}{\Omega_c}\beta_{\perp o}[\gamma_o(\gamma_o-1)]^{1/2}\left(\frac{W_E}{W_{eo}}\right)_{\text{sat}}^{1/2} \text{kV}$$
$$\simeq \begin{cases} 0.12 \text{ kV}, & \text{Case I} \\ 3.35 \text{ kV}, & \text{Case II} \end{cases} \quad (15)$$

The effect of ESCI on the beam distribution function is far greater then implied by the wave saturation level. Fig. 5 shows the evolution of the beam distribution function. As the wave grows, the distribution function broadens. At saturation, a significant fraction of the electrons gain or lose more than 10 percent of the initial kinetic energy.

Fig. 6 shows the time dependence of the electron energy spread, which is defined as the standard deviation $\langle\Delta\gamma\rangle$ normalized to γ_o-1. At saturation, the electron energy spread is

$$\frac{\langle\Delta\gamma\rangle}{\gamma_o-1} \simeq \begin{cases} 9.5 \text{ percent}, & \text{Case I} \\ 8.5 \text{ percent}, & \text{Case II} \end{cases} \quad (16)$$

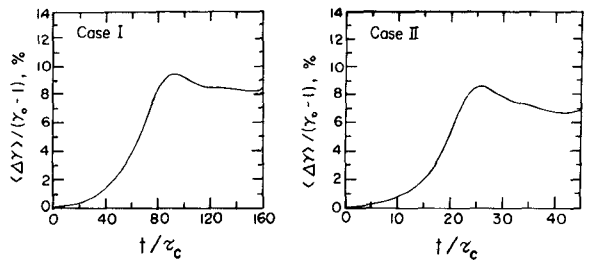

Fig. 6. Energy spread $[\langle\Delta\gamma\rangle/(\gamma_o-1)]$ of the electron beam versus t/τ_c in the small- and large-signal regimes.

D. Physical Interpretation

The two saturation phenomena, large electron energy spread and low wave-energy level, are both the result of energy exchange between the electrons and the wave, but they are governed separately by the individual and collective aspects of the energy exchange.

For simplicity, we take the fundamental harmonic interaction ($n=1$) as an example. The wave frequency ($\Delta\omega$) observed by a gyrating electron is

$$\Delta\omega = \omega - \Omega_e/\gamma$$

where Ω_e is the rest mass electron cyclotron frequency. A relatively large electron energy spread will result under the resonance condition

$$|\Delta\omega| \ll \omega \tag{17}$$

since the inverse of $\Delta\omega$ is roughly a measure of the resonant interaction time (i.e., the duration of *continued* electron energy increase or decrease) between an electron and the wave.

Wave saturation level, however, depends on the net energy lost by *all* the electrons, which is a sensitive function of the sign and magnitude of $\Delta\omega$. If $\Delta\omega \gtrsim 0$, electrons that lose energy will have longer resonant interaction time with the wave than those that gain energy, because $\Delta\omega$ decreases and increases with time for decelerating and accelerating electrons, respectively. As a result, the electrons on average lose energy. The value of $\Delta\omega$ for maximum net electron energy loss (hence maximum wave saturation level), as one might intuitively expect, should be sufficiently large but not too large to violate condition (17). In the normal operation of a gyrotron, ω is determined by the dimensions of the interaction structure while Ω_e is tunable through the applied magnetic field. Hence, $\Delta\omega$ can be tuned to an optimum value to achieve high interaction efficiency [6]. In the case of ESCI, $\Delta\omega$ as given by (8) is typically much smaller than ω and, furthermore, there is little room for tuning. Consequently, electrons can interact strongly with the wave individually, but collectively they give up little energy to the wave.

V. Effects on Gyrotron Performance

As discussed in Section III, the present model does not fully reflect the reality of a gyrotron beam. Neglected in the model are dc space charge effect, geometrical effect, and diffusive beam boundary effect. The following discussion on the gyrotron performance is therefore of a speculative nature, especially where quantitative estimates are concerned.

The ESCI will have its full impact when grown to saturation. Given the fact that the beam has a finite transit time, the level of the initial electrostatic perturbation determines whether saturation will be reached. Let the transit time be $N_c\tau_c$, that is, an electron executes N_c cyclotron rotations in the interaction structure, the total gain can be written

$$G = g_c N_c = 54.6\frac{N_c\omega_t}{\Omega_c}\text{dB} = \begin{cases} 0.48N_c\text{dB}, & \text{Case I} \\ 1.90N_c\text{dB}, & \text{Case II} \end{cases}. \tag{18}$$

Taking the University of Maryland gyroklystron amplifier design [5] as an example, we have $N_c \simeq 13$; hence, Case II of (18) gives $G \simeq 24.7$ dB.

Assuming that the wave grows at the small-signal rate all the way until saturation (a good assumption according to Fig. 4), we can calculate from (14) and (18) the minimum initial electrostatic perturbation that will reach saturation

$$\left(\frac{W_E}{W_{eo}}\right)_{\text{ini}} = 10^{-0.1G}\left(\frac{W_E}{W_{eo}}\right)_{\text{sat}} \simeq \begin{cases} 3.5\times10^{-0.048N_c-4}, & \text{Case I} \\ 1.5\times10^{-0.19N_c-3}, & \text{Case II} \end{cases}. \tag{19}$$

Again, for the University of Maryland design, we find

$$\left(\frac{W_E}{W_{eo}}\right)_{\text{ini}} \simeq 3.4\times10^{-3}\left(\frac{W_E}{W_{eo}}\right)_{\text{sat}} \simeq 5.1\times10^{-6}. \tag{20}$$

From (15) and using the design value of $r_{Lo} = 0.44$ cm, we obtain the corresponding peak electric field

$$E_{\text{ini}} \simeq (3.4\times10^{-3})^{1/2}E_{\text{sat}} \simeq 0.44\text{ kV/cm}. \tag{21}$$

The electron energy spread due to saturated ESCI is 8.5 percent (Case II of (16)). It really does not take this much spread to have a strong effect on the gyrotron performance as the following example will show.

In the normal operation of a gyrotron, the electromagnetic wave modulates the electron energy and thereby causes electron bunching in the cyclotron phase space. The ESCI, if present, spoils the bunching processes by modulating the electron energy at different frequencies. It is interesting to compare the energy spreads due to the electromagnetic and electrostatic waves. For the University of Maryland design, electron energy modulation takes place in three bunching cavities. When operating in the large signal regime, the accumulated electron energy spread in the three bunching cavities is 9.3 percent, a level comparable to that due to the saturated ESCI. Thus, even an unsaturated ESCI could have strong competing effects on the electron bunching processes.

On the other hand, the low saturation level of the ESCI suggests a low noise-to-signal ratio. If the electromagnetic-wave interaction efficiency is 10 percent, for example, the electrostatic noise power would be 24.6 and 18.2 dB below the electromagnetic power for Case I and Case II, respectively. A fraction of the electrostatic noise will be coupled out of the RF channel if $k_z \neq 0$, but the exact amount can not be determined within the scope of the present theory.

In conclusion, we find that the ESCI can create an electrostatic noise spectrum, but its effect will be greater on the saturated gain and efficiency of the gyrotron amplifier than on the noise figure itself.

VI. Summary and Discussion

The level of the initial electrostatic perturbation given by (19)–(21) is likely to originate from, among other causes, the nonuniform emittance of a temperature limited cathode. A different cause, which deserves more serious consideration, is related to the nonuniformity of the interaction structure. When the electron beam propagates from a narrow structure into a wide structure (e.g., from the drift region into a cavity), it will experience a sudden deceleration due to the space charge depression effect [7]. The consequent density fluctuations in the transition region may result in an electrostatic perturbation exceeding the levels in (20) and (21).

The present study demonstrates that these electrostatic perturbations, whether macroscopic or microscopic, will decompose into many electrostatic cyclotron modes to grow within the beam. What makes these modes particularly important is the coincidence of their frequencies with the harmonics of the cyclotron frequency [8]. This allows prolonged acceleration and deceleration of electrons, resulting in a large electron energy spread to spoil the normal electron bunching processes in the gyrotron.

Estimates made in Section V are based on the assumption that the ESCI is convective. If this is true and the applied magnetic field is tapered, the instability may have a much shorter time to grow. But there is also the possibility that the ESCI is absolute (i.e., it grows without propagation). Then, any initial perturbation can grow to saturation. The coupling of the electrostatic modes with the external structure (when $k_z \neq 0$) is also neglected in the present model. A 2-D electromagnetic simulation study including all these effects in a more realistic model seems warranted.

Acknowledgment

The authors wish to express their gratitude to Dr. A. T. Lin and Dr. H. Okuda for their guidance in the development of the code used in the present paper. The authors would also like to thank the Institute of Atmospheric Physics of the National Central University for the privilege of using their computer, and acknowledge many helpful discussions with Prof. J. K. Chao and Prof. F. S. Kuo.

References

[1] P. Charbit, A. Herscovici, and G. Mourier, "A partly self-consistent theory of the gyrotron," *Int. J. Electron.*, vol. 51, pp. 303–330, 1981.
[2] J. L. Hirshfield, "Cyclotron harmonic maser," *Int. J. Infrared Millimeter Waves*, vol. 2, pp. 695–704, 1981.
[3] K. R. Chen and K. R. Chu, "Study of a noise amplification mechanism in gyrotrons," *IEEE Trans. Microwave Theory Tech.*, Jan. 1986.
[4] See, for example, J. M. Dawson and A. T. Lin, "Particle simulation," in Handbook of Plasma Physics, vol. 2, A. A. Galeev and R. N. Sudan, Eds. New York: Elsevier, 1984, ch. 7.1.
[5] K. R. Chu, V. L. Granatstein, P. E. Latham, W. Lawson, and C. D. Striffler, "A 30-MW gyroklystron amplifier design for high-energy linear accelerators," *IEEE Trans. Plasma Sci.*, vol. PS-13, pp. 424–434, 1985.
[6] V. A. Flyagin, A. V. Gaponov, M. I. Petelin, and V. K. Yulpatov, "The gyrotron," *IEEE Trans. Microwave Theory Tech.*, vol. MTT-25, pp. 514–527, 1977.
[7] A. T. Drobot and K. Kim, "Space charge effects on the equilibrium of guided flow with gyromotron," *Int. J. Electron.*, vol. 51, p. 351, 1981, also A. K. Ganguly and K. R. Chu, "Limiting current in gyrotrons," *Int. J. Infrared Millimeter Waves*, vol. 5, pp. 103–121, 1984.
[8] There are other beam modes, such as the ordinary and extraordinary modes, that do not oscillate only at harmonics of the electron cyclotron frequency.

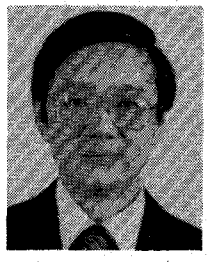

Kwo Ray Chu (SM'82) received the B.S. degree in physics from National Taiwan University in 1965, the M.S. degree in physics from the University of Massachusetts in 1968, and the Ph.D. degree in applied physics from Cornell University in 1972.

From April 1973 to September 1977, he was a Research Physicist with Science Applications, Inc. From September 1977 to September 1983, he was with the U.S. Naval Research Laboratory, serving as Head of the Advanced Concepts Section in the High-Power Electromagnetic Radiation Branch. During this period, he was for three years an Adjunct Associate Professor of Applied Physics at Yale University. Since September 1983, he has been a Visiting Professor in the Department of Physics, National Tsing Hua University, Taiwan, Republic of China. He also has been a Consultant to Science Applications International Corporation since September 1983. Dr. Chu specializes in microwave theory, relativistic electronics, plasma physics, and controlled thermonuclear fusion.

He was elected a Fellow of the American Physical Society in 1983.

Ling-Hsiao Lyu was born in Taiwan. She received the B.S. and M.S. degrees in atmospheric physics from National Central University in 1981 and 1983, respectively. Her master's thesis was on particle simulation of space plasma phenomena.

From 1981 to 1984, she was a research assistant at the Institute of Atmospheric Physics, National Central University. In 1985, she worked as a research assistant in the Department of Physics, National Tsing Hua University. She is currently a graduate student in the Department of Space Physics and Atmospheric Science, University of Alaska Fairbanks.